

Rare regions of the SIS model on Barabási-Albert networks

Géza Ódor

Research Centre for Natural Sciences, Hungarian Academy of Sciences,
MTA TTK MFA, P. O. Box 49, H-1525 Budapest, Hungary

(Dated: December 17, 2018)

I extend a previous work to susceptible-infected-susceptible (SIS) models on weighed Barabási-Albert scale-free trees. Numerical evidence is provided that phases with slow, power-law dynamics emerge as the consequence of quenched disorder in topologies previously studied with Contact Process. I compare simulation results with a spectral analysis of the networks and show that the quenched mean-field (QMF) approximation provides a reliable, relatively fast method to explore activity clustering. This suggests that QMF can be used for describing rare-region effects and smeared phase transitions due to network inhomogeneities. Finite size study of the QMF shows the expected disappearance of the epidemic threshold λ_c in the thermodynamic limit and suggest a nontrivial mean-field behavior characterized by the order parameter $\beta = 2$. This means that the order parameter of the infection $\rho(\lambda)$ vanishes tangentially at the $\lambda_c = 0$ transition point. Application of this method to other models may reveal interesting rare-region effects, Griffiths Phases as the consequence of quenched topological heterogeneities.

PACS numbers: 89.75.Hc, 05.70.Ln, 89.75.Fb

I. INTRODUCTION

The research of nonequilibrium models has been a central research topic of statistical mechanics [1–3]. A fundamental dynamical system model to understand them is the Contact Process (CP) [4, 5], in which sites can be either occupied (infected) or empty (susceptible). By decreasing the infection rate of the neighbors λ/k , where k is the degree of the vertex, a continuous phase transition occurs at some λ_c critical point from active to inactive steady state. The latter is also called absorbing, because no spontaneous activation of sites is allowed and the density of infection (ρ) is zero.

Recently the interest has been shifted from models, defined on Euclidean, regular lattices to processes living on general networks [6, 7]. The effects of the heterogeneous topological structures [8, 9] is not yet fully understood. In particular in the case of ubiquitous scale-free (SF) networks [10], exhibiting $P(k) \sim k^{-\gamma}$ degree distribution of the nodes [6, 7] the location of the phase transition and the singular behavior around is still a debated issue. Numerical simulations [11–14] and theoretical approaches based on the heterogeneous mean-field (HMF) theory [11, 12, 15] show strong effects of the network heterogeneity on the behavior of the CP defined on complex networks.

Although SF-s exhibit infinite topological dimension (d), defined by $N \propto r^d$, where N is the number of nodes within the (chemical) distance r , simple mean-field approximations cannot capture several important features. Studies of the CP, as well as other processes [8, 9] have shown that quenched disorder in networks is relevant in the dynamical systems defined on top of them. Very recently it has been shown, [16–18] that generic slow (power-law, or logarithmic) dynamics is observable by simulating CP on networks with finite d . This observation is relevant for recent developments in dynamical

processes on complex networks such as the simple model of “working memory” [19], brain dynamics [20], social networks with heterogeneous communities [21], or slow relaxation in glassy systems [22].

Slow dynamics can be the consequence of bursty behavior of agents connected by small world networks resulting in memory effects [23]. An independent cause is related to such arbitrarily large ($l < N$), correlated rare-regions (RR), which have long lifetime $\tau \propto \exp(l)$ in the active phase ($\lambda > \lambda_c^0$). In the region $\lambda_c^0 < \lambda < \lambda_c$, a so called Griffiths Phase (GP) [24, 25] develops with an algebraic density decay $\rho \propto t^{-\alpha}$, α being a non-universal exponent. This can only be understood by non-perturbative methods [26–29].

More recently the possibility of such slow dynamics has been investigated on BA networks with $\gamma = 3$ possessing infinite d [30]. Very extensive simulations showed linear leading order density decay and $\rho(\lambda, t \rightarrow \infty) \propto |\lambda - \lambda_c|$ behavior with logarithmic corrections in agreement with the HMF approximations. It was also pointed out that in case of the loop-less BA trees the epidemic propagation slows down, and a nontrivial critical density decay emerges with $\rho(t, \lambda_c) \propto t^{-\alpha}$, $\alpha \simeq 0.5$. Furthermore, when k dependent weighting was also applied, suppressing hubs or making the network disassortative GP-like regions could be observed in the simulations. A systematic finite scaling study revealed that these power-laws saturate in the $N \rightarrow \infty$ thermodynamic limit, suggesting smeared phase transitions [25]. This can be understood because even infinite dimensional RR-s can be embedded in networks with $d = \infty$ causing finite $\rho(t \rightarrow \infty, N \rightarrow \infty)$. A numerical percolation analysis has strengthened this view indeed.

I continue this work [30] to see if quenched mean-field (QMF) theory with spectral decomposition (SD) can help to understand rare-region effects in complex networks. For this reason I study the susceptible-infected-

susceptible (SIS) model [31], instead of the CP because it possesses real symmetric adjacency matrix with positive eigenvalues. The susceptible-infected-susceptible (SIS) model is a two state system, in which infected sites propagate the epidemic (venerate all neighbors) with rate λ , or recover with rate 1.

This extension is far from trivial, because the epidemic transmitting capability of infected nodes is higher, i.e. it is not normalized by the number of outgoing edges. Therefore the emergence of localized rare-regions (RR) is questionable. I provide extensive simulation results showing numerical evidence for GP like regions with slow dynamics similarly as in case of the CP. The QMF and SD analysis set up for these cases is in good agreement with the dynamical simulations.

II. NETWORK MODELS

I consider here SIS on BA networks in particular for loop-less and weighted cases as described in [30]. This permits very simple and fast construction, in contrast with other standard network generation models, e.g [32]. The BA growth starts with a fully connected graph of size $N_0 = 10$ nodes, but comparisons with $N_0 = 5$ and 20 have also been done to test any dependence. For BA at each time step s , a new vertex with m edges is added to the network and connected to an existing vertex s' of degree $k_{s'}$ with probability $\Pi_{s \rightarrow s'} = k_{s'}/\sum_{s'' < s} k_{s''}$. This process is iterated until reaching the desired network size N . The resulting network has a SF degree distribution $P(k) \simeq k^{-3}$. For $m = 1$ we obtain a BA tree (BAT) topology, while for the looped case I applied $m = 3$.

Binary (non-weighted) BA networks can be transformed into weighted ones by assigning to every edge connecting vertexes i and j a symmetric weight ω_{ij} . In [30] two different network topology dependent weight assignment strategy was introduced in order to slow down and localize epidemics.

(i) *Weighted BA tree I (WBAT-I):* Multiplicative weights, suppressing the infection capability of highly connected nodes

$$\omega_{ij} = \omega_0 (k_i k_j)^{-\nu}, \quad (1)$$

where ω_0 is an arbitrary scale and ν is a characteristic exponent with $\nu \geq 0$. This can model internal limitations of hubs, like the sub-linear Heap's law [35]. In this paper I study the case with $\nu = 1.5$ exponent.

(ii) *Weighted BA tree II (WBAT-II):* Disassortative weighting scheme according to the age of nodes in the network construction

$$\omega_{ij} = \frac{|i - j|^x}{N}, \quad (2)$$

where the node numbers i and j correspond to the time step when they were connected the network. Since the degree of nodes decreases as $k_i \propto (N/i)^{1/2}$ during this

process, this selection with $x > 0$ favors connection between unlike nodes and suppresses interactions between similar ones. In [30] simulations showed evidence for a phase with power-law dynamics of the CP for $x = 2, 3$ with CP. This paper is concerned about $x = 2$ networks.

The presence of these weights affects the dynamics of the SIS. Thus, the rate at which a healthy vertex i becomes ill on contact with an infected (active) vertex j is proportional to $\lambda \omega_{ij}$, therefore the epidemic can in principle become trapped in isolated connected subsets. These regions of size l are rare in general: $P(l) \propto \exp(-l)$, but can exhibit exponentially long lifetimes $\tau(l) \propto \exp(l)$. In the healthy (inactive) phase they provide the leading order contribution to the density of infected sites

$$\rho(t) \sim \int l P(l) \exp(-t/\tau) dl, \quad (3)$$

which in the saddle point approximation results in $\rho(t) \sim t^{-\alpha}$ decay [16].

III. SPECTRAL ANALYSIS

In [30] the heterogeneous mean-field (HMF) analysis of CP was worked out for these network models. However, extensive simulations showed different dynamical behaviors, except from the looped BA CP model case. Since HMF can't take into account rare region effects, nor models on trees that conclusion was not very surprising.

A mean-field theory, capable of describing the effects of quenched topologies of the network on which SIS is defined is expected to give better agreement with numerical simulations. The quenched mean-field (QMF) approach is based on the rate equation for $\rho_i(t)$, the infection probability of node i at time t [33]:

$$\frac{d\rho_i(t)}{dt} = -\rho_i(t) + (1 - \rho_i(t)) \sum_j A_{ij} \lambda \rho_j(t), \quad (4)$$

where A_{ij} is an element of the adjacency matrix assigned with 1, if there is an edge between nodes i and j or 0 otherwise. This equation can be generalized by replacing the adjacency matrix with the weighted adjacency matrix $B_{ij} = A_{ij} \omega_{ij}$, having weighted elements $B_{ij} \in [0, 1]$ due to its real symmetry.

For $t \rightarrow \infty$ the system evolves into a steady state, with the probabilities expressed as

$$\rho_i = \frac{\lambda \sum_j B_{ij} \rho_j}{1 + \lambda \sum_j B_{ij} \rho_j}. \quad (5)$$

Stability analysis shows that $\rho_i > 0$ above a λ_c epidemic threshold, with finite order parameter (prevalence) $\rho \equiv \langle \rho_i \rangle$.

In the SD approach one expands ρ_i in the space of eigenvectors of the adjacency matrix A_{ij} (or B_{ij} for weighted case) as

$$\rho_i = \sum_{\Lambda} c(\Lambda) f_i(\Lambda). \quad (6)$$

This extension can be done for real and symmetric weights, when the eigenvectors $\mathbf{f}(\Lambda)$ span a complete orthonormal basis. The Perron-Frobenius theorem asserts that a real square matrix with positive entries has a unique largest real eigenvalue $\Lambda_{max} \equiv \Lambda_1 \geq \Lambda_2 \geq \dots \Lambda_N$ and that the corresponding eigenvector $\mathbf{f}(\Lambda_1)$ has strictly positive components. In this basis Eq. (5) can be expressed by the coefficients $c(\Lambda)$

$$c(\Lambda) = \lambda \sum_{\Lambda'} \Lambda' c(\Lambda') \sum_{i=1}^N \frac{f_i(\Lambda) f_i(\Lambda')}{1 + \lambda \sum_{\tilde{\Lambda}} \tilde{\Lambda} c(\tilde{\Lambda}) f_i(\tilde{\Lambda})}. \quad (7)$$

This gives $\lambda_c = 1/\Lambda_1$ for the epidemic threshold and in its neighborhood the order parameter can be approximated by the eigenvectors of the largest eigenvalues

$$\rho(\lambda) \approx \alpha_1 \Delta + \alpha_2 \Delta^2 + \dots, \quad (8)$$

where $\Delta = \lambda \Lambda_1 - 1 \ll 1$ with the coefficients

$$\alpha_j = \sum_{i=1}^N f_i(\Lambda_j) / [N \sum_{i=1}^N f_i^3(\Lambda_j)]. \quad (9)$$

A homogeneous solution implies that a finite fraction of vertexes are infected right above λ_c and α_1 is the order of $O(1)$. That would mean that the components of $\mathbf{f}(\Lambda_1)$ are localized. On the other hand quenched inhomogeneous topologies can also imply inhomogeneous ρ_i distributions and one can assume that they result in rare region effects, as in [16–18, 30].

To describe localization in the components of $\mathbf{f}(\Lambda_1)$ [33] suggested to use the inverse participation ratio

$$IPR(\Lambda) \equiv \sum_{i=1}^N f_i^4(\Lambda), \quad (10)$$

which in the limit $N \rightarrow \infty$ is of the order of $O(1)$ when the eigenvector is localized. Contrary, when $IPR(\Lambda) \rightarrow 0$ this state is delocalized. Eq. (9) implies that for localized principal eigenvector $\alpha_1 \sim O(1/N)$, thus $\rho \approx \alpha_1 \Delta \sim O(1/N)$, the disease is localized on a finite number $N\rho$ of vertexes. On the other hand, when $\mathbf{f}(\Lambda_1)$ is delocalized the disease infects a finite fraction of vertexes for $\lambda > \lambda_c$.

Goltsev et al. [33] analyzed artificial and real SF networks and found that in case of localized cases the epidemic threshold was actually absent and a real epidemic affecting a finite fraction of vertexes occurred after a smooth crossover at higher values of λ . This is in agreement with the smeared phase transition scenario proposed to explain the numerical results for CP on weighed BA trees in [30]. In those systems rare-regions effects seemed to arise, causing power-law density decays, which ultimately crossed over to saturation to finite ρ -s in the $N \rightarrow \infty$ limit. Right above λ_c similar concave shaped $\rho(\lambda)$ was obtained as in the localized cases of [33]. Here I investigate the situation for SIS instead of CP models, to see if this relation holds on. This has been done using

finite size scaling analysis of the quantities: $\lambda = 1/\Lambda_1$, IPR and α_i for $i = 1, 2, 3$.

It has been proven [34] that for random, unweighted SF networks, with power-law degree distribution $P(k) \propto k^{-\gamma}$ the maximal eigenvalue scales as $\Lambda_1 \propto \sqrt{k_{max}}$ for $\gamma > 2.5$. Furthermore, the maximal degree of the network satisfies $k_{max} = \min [N^{1/2}, N^{1/(\gamma-1)}]$, due to the structural cutoff of a finite network with $\gamma \leq 3$. Therefore, Λ_1 should scale with the network size as

$$\Lambda_1(N) \propto N^{1/4} \quad (11)$$

for $\gamma = 3$ considered here.

Using the software package OCTAVE I generated the B_{ij} matrices of BA, BAT, WBAT-I and WBAT-II networks for several sizes up to $N = 200.000$ and calculated the three largest eigenvalues and the corresponding eigenvectors. From these I deduced $1/\Lambda_1$, IPR and α_i . The whole SD analysis was done using the sparse matrix functions of OCTAVE to handle B_{ij} -s of the networks within reasonable computing times. For the largest sizes 1-2 weeks of a CPU time was needed. Least-squares fitting with the form

$$1/\Lambda_1 = a + b(1/N)^c \quad (12)$$

has been applied for the largest eigenvalues. As Table. I shows a good agreement was obtained with the finite size scaling expectation $\lim_{N \rightarrow \infty} \lambda_c = 1/\Lambda_1 = 0$ of the QMF method. The $N \rightarrow \infty$ extrapolated critical threshold values converge to zero using the three parameter fitting form (12). The fitted power c agrees with exponent of (11) reasonably well, except from the WBAT-I case, where QMF results for only $N \leq 6000$ could be achieved.

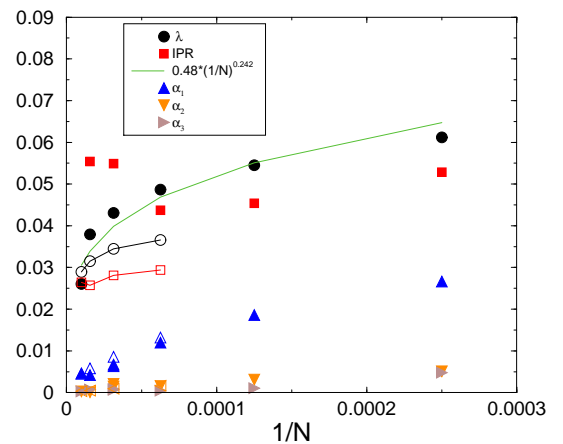


FIG. 1: (Color online) Finite size scaling of QMF SD results for BAT model for $N = 4000, 8000, 16000, 32000, 64000, 100000$. Filled symbols correspond to $N_0 = 10$, hollow ones to $N_0 = 20$. Dashed line: least-squares fitting with the form (12).

The IPR values decrease with $1/N$ and remain very small for the unweighted BA ($IPR < 0.02$) and BAT

TABLE I: Spectral QMF analysis results for SIS in different networks

Network	$1/\Lambda_1$	c	IPR	α_1	α_2	α_3
BA	0.017	0.32	0.014	4×10^{-4}	10^{-7}	10^{-8}
BAT	~ 0	0.24	0.055	10^{-4}	10^{-7}	10^{-9}
WBAT-I	~ 0	0.7	~ 0	$0.36(1)$	15000	19000
WBAT-II	0.001	0.227	0.25	4×10^{-3}	38	24

($IPR < 0.06$) networks, albeit in the latter case the tendency seems to change for $N \geq 32000$ as shown on Fig. 1. This suggests an agreement with the anomalous scaling behavior of CP on the BA tree reported in [30]. Here some clustering may be expected, which should be checked further by studying networks with $N > 10^5$ nodes. Unfortunately this is out of the scope of the present study using OCTAVE, but is in preparation using graphics cards. For the WBAT-II case the IPR stabilizes to $\simeq 0.25(1)$ (see Fig. 2), suggesting a strong epidemic localization.

One can think that the initial compact seeds, from which the BA graphs originate can influence the clustering behavior of the epidemic in the steady state. By varying the seed size: $N_0 = 5, 10, 20$ no measurable effect was found on the WBAT results. For the unweighted BA and BAT networks one can see differences between the finite size results of the $N_0 = 20$ and $N_0 = 10$ cases (see Fig. 1), but the $N \rightarrow \infty$ asymptotic behavior appears to be the same.

More interesting results were found by considering the eigenvectors of the second and third largest eigenvalues. For the unweighted BA and BAT networks one can see $\alpha_1 >> \alpha_2 >> \alpha_3$ in Table I, in agreement with $\beta = 1$ HMF expectations for ρ slightly above the critical threshold. Surprisingly for the weighted WBAT-I and WBAT-II trees the converse appears to be true, the amplitude of the linear term α_1 is much smaller than α_2 and α_3 , though they show large oscillations, and in fact for WBAT-II α_1 vanishes for $N \rightarrow \infty$. Since the order of α_2 and α_3 is the same for all N but much larger than the order of α_1 an unexpected mean-field critical behavior, characterized by the super-linear order parameter exponent $\beta = 2$ emerges for WBAT-II. It is not clear from the present WBAT-I data whether only very strong corrections-to scaling or the same mean-field class appears asymptotically for $N \rightarrow \infty$. In any case plotting $\rho(\lambda)$ with these values one gets a concave curve from above and a tangential approach to λ_c . Such steady state behavior has already been seen by simulations of CP on weighted BA networks [30, 37]. In the next section I compare these QMF results with simulations of SIS on WBAT-I and WBAT-II networks.

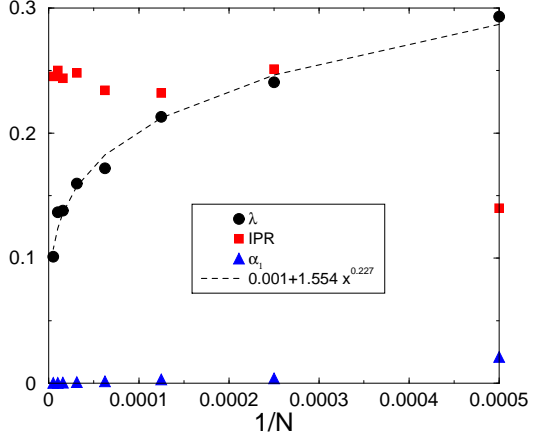


FIG. 2: (Color online) Finite size scaling of QMF SD results for WBAT-II model for $N = 2000, 4000, \dots, 200000$. Solid line: least-squares fitting for with the form (12).

IV. SIS MODEL SIMULATIONS ON WEIGHTED TREES

In simulations I considered the SIS model in continuous time as in [36], to be in accordance with the rate equations. At each time step a randomly chosen infected node recovers with probability $n_i/(n_i + \lambda n_n)$, where n_i is the the number of infected nodes and n_n is the total number of links emanating from them. Complementary, one of its randomly selected neighbor is infected, with probability $\lambda n_i/(n_i + \lambda n_n)$. Following the reaction N_i and N_n are updated and the time is incremented by $\Delta t = 1/(n_i + \lambda n_n)$. The time is measured by these Monte Carlo steps (MCs) and shown to be dimensionless on the figures. These processes are iterated until $t < t_{max}$, or until the epidemic stops ($N_i = 0$).

The networks were generated via the BA linear preferential attachment rule [10], following an initial fully connected seed of $N_0 = 20$. Neighbor indices of sites are stored in a dense matrix to save memory, thus up to $N = 6 \times 10^6$ sized networks could be studied. The initial state was fully active and the concentration of infected sites was followed up to $t_{max} = 4 \times 10^6$ MCs. Density decay runs were repeated and averaged over $\sim 10^4$ and up to 10^5 independent network realizations for WBAT-I and WBAT-II, respectively. The behavior in the active steady state was also investigated by measuring $\rho(\lambda, t \rightarrow \infty)$ deeply in the saturation region.

As Figure 3 shows $\rho(t)$ of the WBAT-I model with $N = 2 \times 10^6$ nodes exhibit λ dependent power-laws for $t > 3 \times 10^5$ MCs in the region $\simeq 37.72 \leq \lambda \leq \simeq 37.77$. The fitted slope of the lowest, $\lambda = 37.72$ power-law curve is: $\alpha \simeq 0.343$. By increasing the size a level-off of these curves can be observed. For $N = 6 \times 10^6$ the steady state values are shown in the inset of Fig. 3. Direct least-squares fitting with the form

$$\rho(\lambda, t \rightarrow \infty) = C(\lambda - \lambda_c)^\beta \quad (13)$$

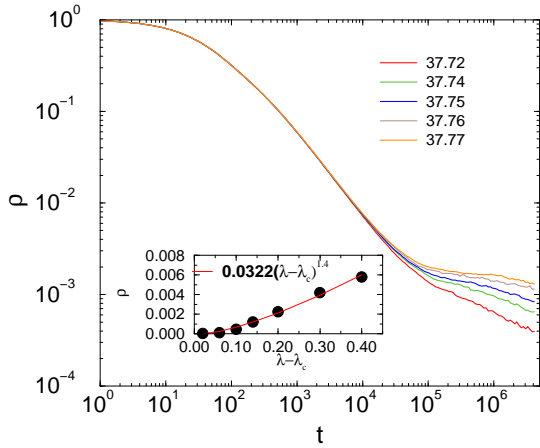


FIG. 3: (Color online) Density decay as a function of time for the SIS model on weighted BA trees generated with the WBAT-I scheme with exponent $\nu = 1.5$. Network size $N = 2 \times 10^6$. Different curves correspond to $\lambda = 37.72, 37.74, 37.75, 37.76, 37.77$ (from bottom to top). Inset: Steady state density (bullets) above the epidemic threshold. The curve shows power-law fitting.

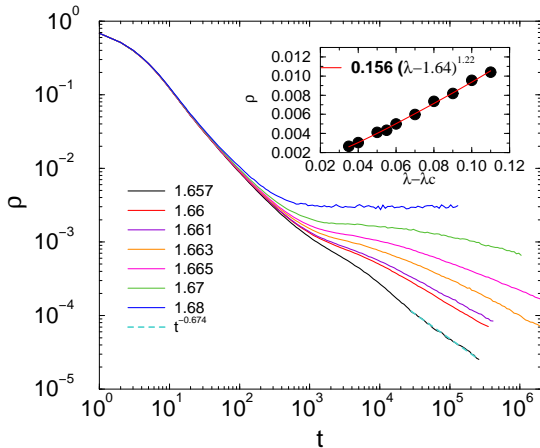


FIG. 4: (Color online) Density decay as a function of time for the SIS on weighted BA trees generated with the age-dependent (disassortative) WBAT-II scheme with exponent $x = 2$. Network size $N = 10^6$. Different curves correspond to $\lambda = 1.657, 1.66, 1.661, 1.663, 1.665, 1.67, 1.68, 1.69$ (from bottom to top). Dashed line: power-law fit. Inset: Steady state density (bullets) above the epidemic threshold. The curve shows power-law fitting.

results in: $\beta = 1.4(1)$ and $C = 0.0322(5)$, a slower than linear approach to the estimated threshold: $\lambda_c = 37.60(2)$. These results are in agreement with the CP case [30], suggesting again a smeared transition, with $\lambda_c \rightarrow 0$ in the $N \rightarrow \infty$ limit.

In the case of WBAT-II network the power-laws decays of $\rho(t, \lambda)$ appears much earlier, for $t > 50.000$ MCs, and more pronouncedly, albeit corrections to scaling are non-negligible. The slope of the lowest, $\lambda = 1.657$ curve is: $\alpha \simeq 0.674$, obtained by fitting for $t > 20.000$ MCs, which

is far away from the HMF critical exponent: $\alpha = 1$. This region can be found for $\sim 1.657 \leq \lambda < \sim 1.67$, at much lower values as for CP, and I predict a smeared transition again, since the densities in the steady state $\rho(t \rightarrow \infty)$ increase with N . As the inset of Fig. 4 shows $\rho(\lambda, t \rightarrow \infty)$ can be fitted using (13) with an order parameter exponent $\beta = 1.22(1)$ near $\lambda_c = 1.64(1)$ for networks with size ($N = 4 \times 10^6$).

V. DISCUSSION AND CONCLUSIONS

Understanding effects of heterogeneities in nonequilibrium, dynamical systems is a challenging open field. References [16, 18] concluded that finite topological dimension is a necessary condition for observing Griffiths Phases and activated scaling in case of the basic model of nonequilibrium system, the Contact Process. In case of CP on certain weighed networks numerical evidence was shown for generic power-laws, but in the thermodynamic limit this phase seems to disappear and a smeared phase transition exists, due to the infinite dimensional correlated rare-regions [30]. In contrast with these strong disorder renormalization studies of the random transverse-field Ising model found Griffiths singularities [40] even in the infinite dimensional Erdős-Rényi random graphs [41].

Very recently Griffiths phases have been reported in a study of the Random Transverse Ising Model on complex networks with a scale-free degree distribution regularized by an exponential cutoff $p(k) \propto k^{-\gamma} \exp[-k/\xi]$ [38]. This model was devised to understand the relation between the onset of the superconducting state with the particular optimum heterogeneity in granular superconductors. On quenched networks a phase transition at zero temperature and a Griffith phase with decreasing size as the function of the cutoff ξ was found. The scenario is similar to our case, because increasing the value of the cutoff is like going to the thermodynamic limit of the SF network. Another fresh model study [39] argues again for the existence of GP in the SIS model defined on unclustered, deterministic SF networks, with $\gamma > 3$, below the percolation threshold.

In this work I provided spectral decomposition and QMF approximation to SIS models on different scale-free networks. This analysis supplemented by extensive numerical simulations, which also show strong effects of the topological disorder. In particular non-conventional mean-field behavior has been found in case of weighted BA tree models characterized by the order parameter exponent $\beta = 2$. Such mean-field universality class has not been known before [2], HMF predicts $\beta = 1$, although simulations [30, 37] and other numerical data [33] have already shown signs for leading order singularity with $\beta > 1$ order parameter behavior in certain SF networks.

Activity localization of the eigenvectors characterized by the IPR number hints also for strong rare-region effects in case of SIS on the weighted WBAT-II trees. Numerical simulations exhibit an extended λ parameter

region, with continuously changing power-laws decays. Still, in the $N \rightarrow \infty$ limit the $\rho(t)$ curves saturate, as in case of smeared phase transitions, argued in [30]. For the WBAT-I tree the picture is less clear. There is again a narrow GP like region at very late times ($t > 3 \times 10^5$ MCs), but the $\rho(t)$ curves seem to exhibit strong corrections to power-laws [42]. The SD QMF analysis could be performed up to $N = 6000$ nodes here, and the vanishing IPR obtained by the extrapolation is less certain.

This study goes one step further as [33] by analyzing spectral data of different graphs via finite size scaling. In particular numerical evidence is shown for the disappearance of λ_c with the expected scaling law in the $N \rightarrow \infty$ limit. Fluctuations, omitted by the QMF approximation can be relevant, indeed $\lambda_c > 0$ obtained by simulations of SIS on finite graphs. However, finite size study suggest $\lambda_c = 0$ in all cases, in accordance with smeared

phase transition. Still the QMF SD analysis seems to be a relatively fast, promising way to explore topological rare-region effects, GPs in networks, especially with infinite topological dimension. Extension of this method for using more powerful numerical techniques is under way.

Acknowledgments

I thank R. Pastor-Satorras, R. Juhász and I. Kovács for useful discussions and acknowledge support from the Hungarian research fund OTKA (Grant No. T77629), HPC-EUROPA2 (pr. 228398) and the European Social Fund through project FuturICT.hu (grant no.: TAMOP-4.2.2.C-11/1/KONV-2012-0013).

[1] J. Marro and R. Dickman, *Nonequilibrium Phase Transitions in Lattice Models* (Cambridge University Press, Cambridge, 1999) .

[2] G. Ódor, *Universality in Nonequilibrium Lattice Systems* (World Scientific, Singapore, 2008).

[3] M. Henkel, H. Hinrichsen, and S. Lübeck, *Nonequilibrium phase transition: Absorbing Phase Transitions* (Springer Verlag, Netherlands, 2008).

[4] T. E. Harris, Ann. Prob. **2**, 969 (1974).

[5] T. M. Liggett, *Interacting Particle Systems* (Springer-Verlag, New York, 1985).

[6] R. Albert and A.-L. Barabási, Rev. Mod. Phys. **74**, 47 (2002).

[7] S. N. Dorogovtsev and J. F. F. Mendes, *Evolution of networks: From biological nets to the Internet and WWW* (Oxford University Press, Oxford, 2003).

[8] S. N. Dorogovtsev, A. V. Goltsev, and J. F. F. Mendes, Rev. Mod. Phys. **80**, 1275 (2008).

[9] A. Barrat, M. Barthélémy, and A. Vespignani, *Dynamical Processes on Complex Networks* (Cambridge University Press, Cambridge, 2008).

[10] A.-L. Barabási and R. Albert, Science **286**, 509 (1999)(Oxford University Press, Oxford, 1992) .

[11] C. Castellano and R. Pastor-Satorras, Phys. Rev. Lett. **96**, 038701 (2006).

[12] C. Castellano and R. Pastor-Satorras, Phys. Rev. Lett. **100**, 148701 (2008).

[13] S. C. Ferreira, R. S. Ferreira, and R. Pastor-Satorras, Phys. Rev. E **83**, 066113 (2011).

[14] S. C. Ferreira, R. S. Ferreira, C. Castellano, and R. Pastor-Satorras, Phys. Rev. E **84**, 066102 (2011).

[15] M. Boguñá, C. Castellano, and R. Pastor-Satorras, Phys. Rev. E **79**, 036110 (2009).

[16] M. A. Muñoz, R. Juhász, C. Castellano, and G. Ódor, Phys. Rev. Lett. **105**, 128701 (2010).

[17] G. Ódor, R. Juhász, C. Castellano, and M. A. Muñoz, in *Nonequilibrium Statistical Physics Today*, Vol. 1332, edited by P. L. Garrido, J. Marro, and F. de los Santos (AIP, 2011) pp. 172–178.

[18] R. Juhász, G. Ódor, C. Castellano, and M. A. Muñoz, Phys. Rev. E **85**, 066125 (2012) .

[19] S. Johnson, J. J. Torres, and J. Marro, *arXiv* : 1007.3122

[20] D. R. Chialvo, *Criticality in Neural Systems*, Niebur E, Plenz D, Schuster HG. (eds.) *John Wiley & Sons* (2013), arXiv:1210.3632

[21] X. Castelló, R. Toivonen, V. M. Eguíluz, J. Saramäki, K. Kaski and M. San Miguel, EPL **79** (2007) 66006.

[22] A. Amir, Y. Oreg, and Y. Imry, Phys. Rev. Lett. **105**, 070601 (2010).

[23] M. Karsai, et al. Phys. Rev. E **83**, 025102(R) (2011).

[24] R. B. Griffiths, Phys. Rev. Lett. **23**, 17 (1969).

[25] T. Vojta, Journal of Physics A: Mathematical and General **39**, R143 (2006).

[26] A. J. Bray, Phys. Rev. Lett. **59**, 586 (1987).

[27] D. Dhar, M. Randeria, and J. P. Sethna, Europhys. Lett. **5**, 485 (1988).

[28] H. Rieger and A. P. Young, Phys. Rev. B **54**, 3328 (1996).

[29] D. S. Fisher, Phys. Rev. Lett. **69**, 534 (1992).

[30] G. Ódor and R. Pastor-Satorras, Phys. Rev. E **86**, (2012) 026117.

[31] R. M. Anderson and R. M. May, *Infectious diseases in humans*, (Oxford University Press, Oxford, 1992).

[32] M. Catanzaro, M. Boguñá, and R. Pastor-Satorras, Phys. Rev. E **71**, 027103 (2005).

[33] A. V. Goltsev, S. N. Dorogovtsev, J. G. Oliveira, and J. F. F. Mendes, Phys. Rev. Lett. **109**, 128702 (2012)

[34] F. Chung, L. Lu and V. Vu, Proc. Natl. Acad. Sci. USA **100** 6313 (2003)

[35] H. Heaps, *Information retrieval: Computational and theoretical aspects* (Academic Press, Inc. Orlando, FL, USA, 1978).

[36] S. C. Ferreira, C. Castellano, R. Pastor-Satorras, Phys. Rev. E **86**, 041125 (2012)

[37] M. Karsai, R. Juhász, and F. Iglói, Phys. Rev. E **73**, 036116 (2006).

[38] G. Bianconi, J. Stat. Mech. (2012) P07021.

[39] H. K. Lee, P.-S. Shim and J. D. Noh, *arXiv*:1211.2519.

[40] I. A. Kovács, F. Iglói, J. Phys.: Condens. Matter **23** (2011) 404204.

[41] P. Erdős, A. Rényi, Publicationes Mathematicae **6**, 290 (1959).

[42] Note, that logarithmic corrections to scaling are well known in the GP [25].